High-Frequency, Steel-Flexure, Acoustic-to-Electric Transducer for Cryocoolers

Thomas W. Steiner

Etalim Inc.
Vancouver, BC, V5Y1M7, Canada

ABSTRACT

A steel flexure acoustic to electric transducer developed for a thermoacoustic engine is proposed for use as a driver for cryocoolers. This transducer operates at around 500 Hz and will thus allow for the construction of simpler, more reliable, more compact, and higher power density cryocoolers. The transducer characteristics are high efficiency (87%), high power (1 kW), lack of sliding parts, and very long maintenance of free life. The transducer uses a moving iron only flux switching alternator to allow for efficient small motion actuation. Furthermore, the alternator is external to the pressure vessel, and thus, there is no possibility of contamination of the working gas by outgassing. Simulation results of a 77 K cryocooler using such a transducer with thermoacoustic code vetted on an engine are very competitive with a Stirling cryocooler.

INTRODUCTION

A steel diaphragm, acoustic-to-electric transducer built for use with thermoacoustic engines, has properties that make it an ideal candidate for cryocooler use. We start with a description of the transducer operation, list its specifications, and then explain this transducer's characteristics that make it ideal for use with high reliability cryocoolers. The transducer properties require that a cryocooler using this transducer will have to operate at high frequency (400-500 Hz), but this is not inherently a problem as we have demonstrated successful thermoacoustic engine operation at these frequencies. Higher frequency operation will result in higher power density and more compact cryocoolers. Radebaugh [1,2] has identified high-frequency cryocooler operation as a potential path forward to building improved cryocoolers.

We present a schematic of a proposed cryocooler apparatus using such a transducer and other thermoacoustic components previously vetted in a thermoacoustic genset. Simulation results of the proposed cryocooler are presented that indicate expected performance will be very competitive with free-piston Stirling cryocoolers operating across the same temperature difference. The acoustic simulation code used was previously successfully used to design and accurately model thermoacoustic engines, so it is reasonable to assume it will also accurately simulate cryocooler performance. Our custom simulation code uses the same mathematics and general method as the freely available thermoacoustic simulation software DeltaEC [3,4] but has features specifically tailored for use with our transducers and other thermoacoustic components.

Cryocoolers 21, edited by R.G. Ross, Jr., J.R. Raab and S.D. Miller

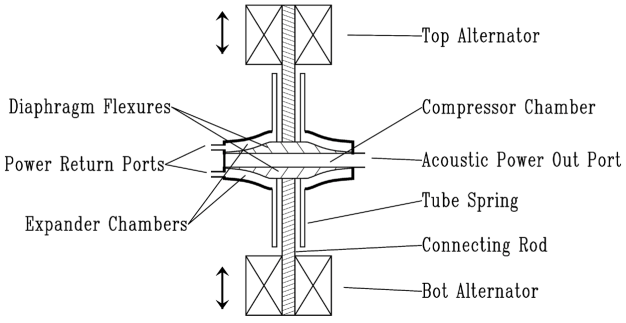

Figure 1. Steel flexure transducer schematic.

PRINCIPLE OF OPERATION

As seen in the schematic diagram of Figire 1, the transducer consists of two back to back diaphragms that define a compressor chamber between them. A side port provides a means for generated acoustic power to flow out of the chamber into a transmission duct connected to the transducer. The volumes between the other sides of the diaphragms and the pressure vessel housing together form a joint expander volume provided that the two expansion chambers are fluidically connected. The most novel feature of this transducer are the tube springs. The tube springs in the schematic consist of two thin wall tubes, one within the other, joined at the distal ends and with the inner proximal end connected to the diaphragm and the outer proximal end connected to the housing. Thus, the tube spring walls form part of the pressure vessel, and the alternators are outside of the pressure vessel. Such a tube spring is lightweight yet exceedingly stiff as it works by axial compression and extension of the thin wall tubes. The range of motion is small but matches the maximum diaphragm flexure motion amplitude of 200 μm. The tube springs allow the mechanical vibration power to be coupled out of the pressure vessel without dynamic seals and allows the transducer pressure vessel to be hermetically sealed. The tube springs raise the transducer's mechanical resonance frequency into the 400 – 500 Hz range even with several kilograms of flux switching alternator mass connected to the diaphragms utilizing the connecting rods within the central bore of the tube springs. Not shown in the schematic are the alternator details, but the alternators [5] consist of two parts. The stationary part is attached to the transducer housing and consists of a permanent magnet, electrical steel pole pieces, and the coils. The second component is a vibrating reciprocator consisting of electrical-steel flux-path closing pieces attached to the connecting rod.

Raising the transducer's frequency compensates for the small flexure range of motion such that the power density can be competitive with that of piston transducers. An additional consequence of the very stiff tube spring is that the connecting rods between the diaphragms and the alternator reciprocators cannot be considered infinitely stiff compared to the tube spring. Thus, a multi-mass coupled oscillator model is needed to understand the detailed transducer dynamics [6]. Such a model predicts that when the diaphragm amplitude is 200 μm, the reciprocator motion amplitude is ~340 μm dependent in part on the working gas spring contribution.

We have previously used such transducers to build natural gas fired thermoacoustic gensets characterized by very long maintenance-free lifetimes [7-9]. The measured transducer electrical to mechanical efficiency at 1 kW of alternator electrical power is 87% [6], which is considerably better than the efficiencies of piston transducers tabulated by Timmer [10] and by Wakeland [11]. The bulk of the full power losses are electrical losses rather than mechanical losses, and thus, 95% efficiency is in principle possible if the flux switching linear alternators [5] are sized to optimize efficiency rather than cost.

TRANSDUCER ADVANTAGES FOR CRYOCOOLERS

Table 1 contains the transducer specifications. The electrical values assume that the top and bottom alternators are wired in parallel. Higher voltage and lower current operation may be obtained

Table 1. Transducer specifications.

Feature	Value	Units
Alternator peak electric drive power	1200	W
Transducer efficiency	91% @ 300W, 87% @1000W	%
Frequency	400-500	Hz
Diameter (not including ports)	250	mm
Height	550	mm
Mass	~30	kg
Design mean working gas pressure	12	MPa
Peak differential pressure across diaphragm (phase dependent)	0.7-1.0	MPa
Alternator inductance (both in parallel)	44	mH
Alternator winding resistance (450 Hz effective)	6.28	Ω
Transducer mechanical resistance	48	Ns/m
Transducer force constant	361	N/A
Peak alternator current amplitude	~7	A
Design life (continuous operation)	> 10	years
Manufacturing cost @ 5000 / year	~800	USD
Vibration balanced	Yes	
Double acting	Yes	
Hermetically sealed	Yes	

by wiring the alternators in series, in which case some of the electrical parameters will be different. In practice, it is necessary to tune out the winding inductive reactance by adding an external, frequency-dependent tuning capacitor. A suitably chosen tuning capacitor reduces the driver voltage needed for a given current, minimizes the current needed to reach a given diaphragm amplitude, and prevents the forces due to the current from shifting the transducer resonant frequency.

The characteristics of this steel flexure transducer that make it an ideal driver for cryocoolers are itemized in Table 2. The use of diaphragms and tube springs avoids the need for sliding parts, clearance seals, and lubricants. This results in zero wear, thus zero debris formation, and makes the transducer immune to seizing due to temperature gradients. It avoids the need for very tight tolerance machined parts. The lack of clearance seal also avoids any appendix gap losses or the possibility of leakage flow around the piston. The transducer is hermetically sealed to ambient as there are no polymer seals or feedthroughs, only welded seals, and thus no possibility of working fluid leakage provided there are no weld pinholes or other defects. The alternators are moving iron only, so the failure modes associated with moving coils or moving magnets are avoided. Very low mechanical losses allow this transducer to be higher efficiency than competing piston transducers.

The transducer mechanical resonance frequency is inherently high due to the stiffness of the tube springs. The high frequency compensates for the diaphragm flexure's limited range of motion and,

Table 2. Benefits of this transducer for use with cryocoolers.

Characteristic	Benefit
Lack of sliding parts	**No** wear, debris, thermal deformation failure
Lack of dynamic seals	**No** wear, debris, Gedeon streaming, lubricants
Alternators out of pressure vessel	**No** electrical feedthroughs, organic outgassing, heavy PV
Lack of moving coils	**No** electrical lead fatigue
Lack of moving magnets	**No** adhesive detachment, magnet breakup
Only metallic interior surfaces	**No** outgassing or significant surface desorption
Hermetic welded seals only	**No** working fluid leakage
Lack of clearance seal leading to hermetic seal between chambers	**No** very tight tolerance machined parts, clearance gap losses, Gedeon streaming.
High-frequency operation	**No** excessively large components required
Peak alternating stress < 240 MPa	**No** fatigue failure for > 10 years of continuous operation

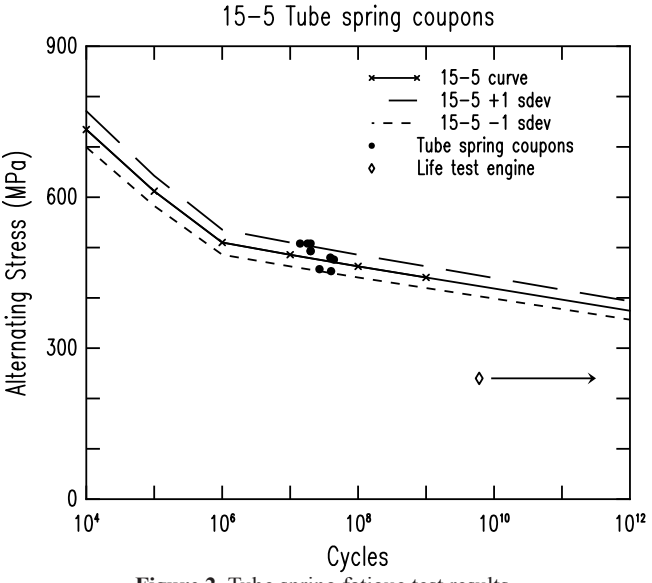

Figure 2. Tube spring fatigue test results.

as the 500 Hz sound wavelength in helium is only about 2 m, allows for compact thermoacoustic apparatus with short, and hence, low loss connecting ducts. A short duct allows for the efficient feedback of unused acoustic power with the right phase to the chambers on the diaphragms' back sides. The transducer is inherently double-acting and hermetically sealed between the two chambers so that there is no possibility of Gedeon streaming [12] with the transducer used in a looped device.

There are additional cryocooler specific advantages of this transducer. Since the alternators are outside the pressure vessel, there are no adhesives or other organic materials associated with the alternators within the pressure vessel, and thus no organic outgassing that could freeze out at the low-temperature end of the cryocooler. Also, as all the seals are welded metal seals, there are no organics associated with O-rings or feedthroughs. All the transducer's interior surfaces in contact with the working gas are easy to clean metal surfaces, thereby limiting the amount of surface desorption working gas contamination that can occur.

FATIGUE TEST RESULTS

A natural question mark for flexure transducers is fatigue failure. In this transducer, the components that experience the largest alternating stresses are the tube springs. These springs and the diaphragms are fabricated from 15-5 precipitation hardening stainless steel, known to have outstanding high cycle fatigue characteristics [13]. Given the high operating frequency, a vast number of cycles are required to achieve ten years or more of continuous operation. Fortunately, the peak allowed stress only drops about 5% per decade in the gigacycle fatigue regime and thus, achieving long life is a matter of designing the components so that the peak alternating stress is well below the fatigue failure stress at a desired number of cycles. Figure 2 shows accelerated life test results on tube spring coupons tested to failure by running them at higher stress. The known 15-5 fatigue curve was shifted down slightly to match the mean of the test coupons. This shift is consistent with a small surface finish derating, or else it may be compensating for small sensor calibration errors. The open diamond's y-axis position corresponds to the design peak alternating stress of 240 MPa. The x-axis position is approaching 10^{10} cycles corresponding to a test thermoacoustic engine using such a transducer that has to date run about 4000 hours and is continuing to accumulate hours. The design stress is well below the fatigue limit, leaving a considerable margin for statistical variation or small machining defects. Thus, there is reason to believe with a high degree of certainty that the transducer will reach at least ten years of continuous operation at 1.6×10^{11} cycles. In all likelihood, it will survive much longer than that.

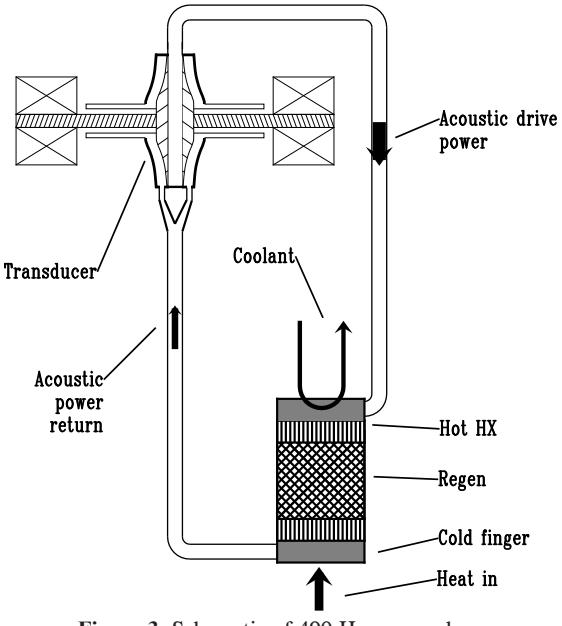

Figure 3. Schematic of 490 Hz cryocooler.

PROPOSED 490 HZ THERMOACOUSTIC CRYOCOOLER

The advantage of a pulse tube cryocooler over a free-piston Stirling cryocooler is the lack of a cold sliding displacer, thereby reducing the possible failure modes and simplifying the apparatus. The disadvantage is a slightly lower performance for medium temperature cryocoolers due to dissipating the unused acoustic power rather than recycling it [14]. The next logical step for further simplification, reliability improvements, and cost reduction is eliminating the ambient temperature sliding pistons. This may be done with our flexure transducer, which at the same time also allows for unused acoustic power to be recycled so that efficiency is simultaneously improved.

Figure 3 is a schematic of the proposed system. Acoustic power generated by the diaphragms' motion in the transducer's central compressor chamber is ducted to the thermal module ambient temperature side by a tuned duct. The thermal module consists of an ambient temperature exchanger, regenerator, and a cold exchanger. The ambient heat exchanger exchanges heat between the working gas and a circulating coolant. Pure passive cooling of this exchanger is also possible using water heat pipes. The cold heat exchanger transfers conductive heat input from a cold finger integrated into the heat exchanger to the working gas. Both heat exchangers are of a design previously used for thermoacoustic engines where the heat flow direction is axial in order to use a larger area and shorter length to minimize temperature deltas for the heat flow path [15]. The acoustic power ports are to the side, and the acoustic flows undergo a 90-degree change of direction within the heat exchangers. This type of heat exchanger has been proven in use with our high-frequency and high-pressure thermoacoustic engines. Sandwiched between the heat exchangers is the regenerator disposed within a thin wall stainless steel pressure vessel sleeve to minimize the parasitic heat flow into the cold end. Any remaining acoustic power exiting the cold end is ducted back to other sides of the diaphragms to be efficiently recycled. Since the frequency is high, the return duct is short, and the power losses minimal, thereby allowing almost all the unused power to be reused. Part of the return duct is tapered in the simulation to form a buffer tube but is not explicitly drawn in the schematic as the taper needed is very slight. A buffer tube may not be needed in practice as the return duct is long enough to thermally isolate the cold finger end of the thermal module from the transducer. However, without a defined buffer tube with an ambient temperature thermal anchor the optimal length of the return duct may be slightly different.

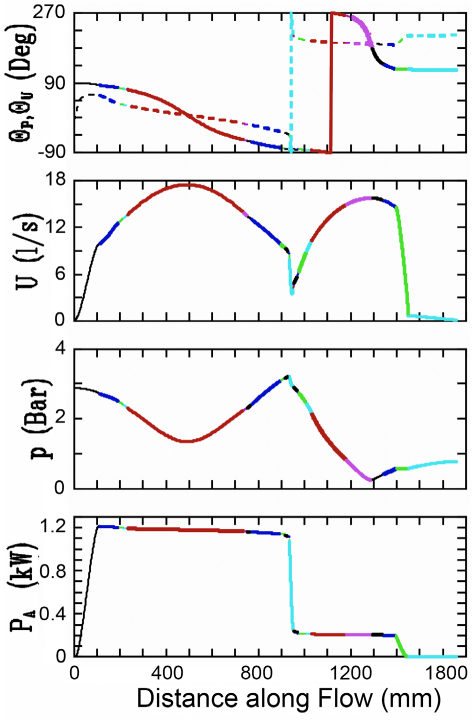

Figure 4. Simulation results for 490 Hz cryocooler.

SIMULATION OF A 490 HZ THERMOACOUSTIC CRYOCOOLER

Performance of the proposed cryocooler may be simulated using DeltaEC [3,4] like thermoacoustic modelling, the results of which are shown in Figure 4. The bottom-most graph of Figure 4 is the simulated acoustic power around the loop. The numerical integration starts in the center compressor chamber and proceeds along the acoustic path in the apparatus until the diaphragms' far side is reached. The system consists of a series of segments, each with a linear extent with the color changes in the graph corresponding to different segments. Phases of the pressure swing and volumetric flow are shown in the top graph of Figure 4, while the middle graphs show the pressure and flow amplitudes as a function of position along the length of the loop. The driven diaphragms' motion initially produces acoustic power in the compressor chamber, which corresponds to the initial rise in power leftmost in the graph. This power then travels along the compression duct with little loss of power to the thermal unit. In the regenerator, the acoustic power drops rapidly as the power is converted into a temperature lift of the input heat. The remaining acoustic power at the cold end is then ducted back to the transducer with very little loss to be reabsorbed by the diaphragms' motion on the expander side. The duct lengths and diameters are tuned so that the phasing everywhere is optimal. An additional pre-fabrication handle that allows transducer acoustic impedance adjustments is changing the chamber heights on one or both of the diaphragm's compressor and expander sides. Varying the chamber heights does not affect transducer dynamics but modifies the acoustic impedance seen at the transducer ports. It was necessary to substantially increase the expander chamber's height from what was optimal for a thermoacoustic engine to obtain the results in Figure 4.

It was also necessary to decrease the mean working gas pressure from 12 to 4 MPa to keep the input power below 1200 W at the alternators. The reduced mean pressure resulted in a simulated pressure amplitude of only about 0.25 MPa across the diaphragms. The diaphragms can handle at least three times this differential pressure. Thus, the transducer's mechanical components, sized as built for an engine, could handle about three times greater acoustic power if equipped with higher power alternators. Note that with the transducer used with an engine, there is much more circulating

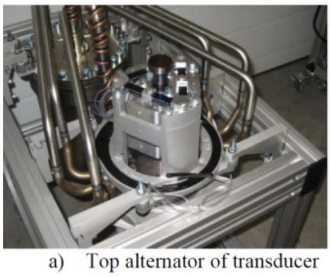

a) Top alternator of transducer

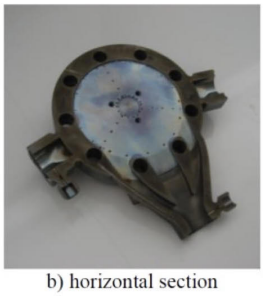

b) horizontal section

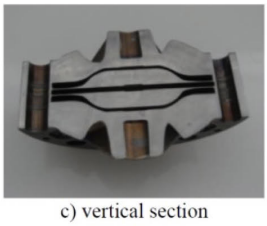

c) vertical section

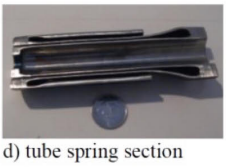

d) tube spring section

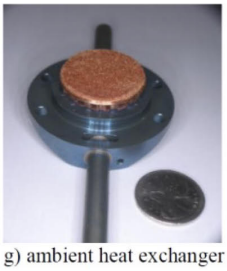

g) ambient heat exchanger

e) 250 W thermal module

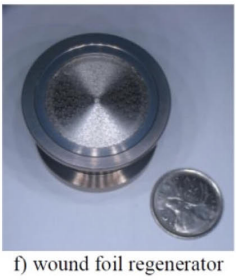

f) wound foil regenerator

Figure 5. Various 450 Hz thermoacoustic engine parts also suitable for cryocooler use.

acoustic power, and the alternators are only sized for the difference between input and output powers in the two chambers. Thus, with modest additional cost, a similar-sized transducer operating at higher mean pressure and equipped with larger alternators could produce 3 kW of acoustic drive to a cryocooler rather than the 1 kW simulated.

The simulated thermal module components are very similar to the ones used in our thermoacoustic engines. One thermal module end is near ambient temperature in both applications, and the ambient heat exchanger and interface to the coolant are unchanged. For an engine, the high temperature heat input end requires the use of superalloys, which tend to have low thermal conductivity making it very difficult to conduct heat into a thermal module while maintaining pressure vessel integrity. In contrast, a cryocooler has a cold finger end so that the entire cold end may be copper, which significantly simplifies construction and minimizes temperature gradients.

The average regenerator working gas temperature in a cryocooler is much lower than in an engine. Thus, an optimized regenerator for a cryocooler has a smaller hydraulic radius than one optimized for an engine. In this particular simulation, the greater mean gas density due to lower mean temperature in the regenerator is offset by the reduced mean working gas pressure. The temperature difference between hot and cold ends is much less in a cryocooler than in an engine. Thus, the optimized regenerator length is shorter in a cryocooler than in an engine. Nevertheless, the cryocooler optimized regenerator geometry is within range of the manufacturing techniques previously used to build engine regenerators.

Figure 5 has pictures of various components used in high frequency thermoacoustic engines. These proven components form the basis for the cryocooler simulation with only some small changes in characteristic geometry. Picture a) shows the top alternator of a transducer with sound isolation can removed installed as part of a thermoacoustic engine. Ducts carrying acoustic power connecting the transducer (foreground) to a thermal amplifier module (background) are visible. Pictures b) and c) are horizontal and vertical sections of the transducer. Section b) is horizontal through the compressor chamber and the acoustic power out port is facing towards to bottom right. Two acoustic power

Table 3. Simulation results.

Parameter	Value	Units
Cold finger temperature	77	K
Ambient exchanger temperature	300	K
Refrigeration power	114	W
Ambient heat rejected in coolant	990	W
Transducer electrical drive	1198	W
Mean He pressure	4	MPa
Operating frequency	490	Hz
COP	0.095 (27% of Carnot)	
Round trip path length	1.6	m

return ports are seen at the sides and these feed the expander chambers. Section c) is a vertical section showing the top and bottom diaphragms and the chambers formed between the diaphragms and pressure vessel housing. Picture d) is a lengthwise sectioned tube spring but of a previous design generation. Picture e) is a 250 W engine thermal module with the ambient temperature side at the bottom and electrically heated hot side at the top. This is a test unit and actual engine thermal modules are heated with a natural gas burner. Acoustic power in and out ducts are visible on the right side. Acoustic power flows undergo a 90 degree turn in the heat exchangers. Figure 5, picture g) is an ambient temperature heat exchanger assembly and picture f) is an etched-foil, spiral-wound regenerator in an Inconel sleeve. Such a regenerator separates the hot and cold sides of a thermal amplifier like the one in Figure 5 picture e). An actual 1 kW engine as shown in Figure 5 a) uses 6 thermal amplifiers similar to Figure 5 picture e) in parallel.

Table 3 contains a summary of the simulation results. Parasitic heat loads and heat exchanger temperature deltas are included in the simulation. The predicted results are excellent compared to the known efficiency values for many cryocoolers operating at a similar temperature (Figure 3 of Radebaugh [1]), and thus skepticism is warranted. However, note that the same code simulating substantially the same parts but used as an engine does a good job predicting the measured power and efficiency of our thermoacoustic engines [8,9]. Partly the excellent simulated performance is due to this transducer's very high efficiency, which is not in doubt and will be the same for a cryocooler as for an engine. There is also the lack of any appendix gap losses due to the absence of a piston clearance seal. Acoustic losses are relatively low due to the short connecting duct lengths enabled by the high frequency. However, the simulation assumes zero streaming related losses, which may not be entirely realizable in practice. There is no possibility of Gedeon streaming [4,12] around the loop as the diaphragms prevent any steady flow around the acoustic loop. However, there are other possible streaming mechanisms, for example, Rayleigh streaming in the buffer tube [4,16] or streaming within the regenerator [4,17,18] which, if present, would reduce the performance below the tabulated simulation results. Such streaming needs to be suppressed with detailed component and system design as was done for our thermoacoustic engines. It may well be the case that these possible streaming mechanisms are more difficult to control in a cryocooler than an engine [18] and also that a given amount of streaming is more detrimental to a cryocooler than an engine. Streaming thus presents the most significant risk to the simulation results' validity in predicting actual device performance. Streaming suppression might require additional work or different strategies in a cryocooler application. Assuming that streaming can be substantially eliminated, there is reason to believe that performance close to the simulation results will be achievable when such a cryocooler is eventually built.

CONCLUSIONS

The characteristics of an electric to mechanical transducer previously used for a thermoacoustic engine seem to be ideal for cryocooler use. A cryocooler using such a transducer can be expected to have far fewer possible failure modes and thus a longer maintenance-free lifetime and be of lower cost. A cryocooler using such a transducer must operate a higher frequency than what is usual

for cryocoolers, but this has the advantage of potentially making the device more compact as the acoustic wavelength is then short. The high operating frequency requires different heat exchanger and regenerator components, but these may also be adapted from what has already been developed for high frequency thermoacoustic engines. Simulation results for a cryocooler using this high frequency flexure transducer and matching heat exchanger and regenerator components suggest that excellent performance is achievable.

REFERENCES

1. R. Radebaugh, "Cryocoolers: the state of the art and recent developments," *J. Phys.: Condensed Matter*, Vol. 21 (2009), p. 164219.
2. R. Radebaugh and A. O'Gallagher, "Regenerator operation at very high frequencies for microcryocoolers," *Adv. Cryog. Eng,* Vol. 51 (2006), p. 1919.
3. B.Ward, J. Clark, and G. Swift, "DeltaEC users guide," (2019), www.lanl.gov/thermoacoustics.
4. G. W. Swift, "Thermoacoustics A Unifying Perspectivefor Some Engines and Refrigerators*," 2*nd ed*.,* ASAPress/Springer (2017).
5. K. B. Antonelli, G. D. S. Archibald, R. J. Biffard, K. T. Gottfried, D. B. Jelstad, T. Kanemaru, B. Medard de Chardon, S. J. Smullin, and T. W. Steiner, "Electromechanical transducer apparatus for converting between mechanical and electrical energy," US patent 10,122,250 (2018).
6. T. W. Steiner, K. B. Antonelli, G. D. S. Archibald, B. De Chardon, K. T. Gottfried, M. Malekian, and P. Kostka, "A high frequency, power, and efficiency diaphragm acoustic-to-electric transducer for thermoacoustic engines and refrigerators," submitted to *J.Acoust. Soc. Am.* (2021).
7. T. Steiner and B. De Chardon, "Evolution of a diaphragm beta Stirling engine into a displacer-less thermoacoustic design," *17th International Stirling Engine Conference,* (2016), pp. 253-262
8. M. Elferink and T. Steiner, "Thermoacoustic wasteheat recovery engine. Comparison of simulation and experiment," *Proc. Mtgs. Acoust.,* Vol. 35 (2018), p. 065002.
9. T. W. Steiner, M. Hoy, K. B. Antonelli, M. Malekian, G. D. S. Archibald, T. Kanemaru, W. Aitchison, B. De Chardon, K. T. Gottfried, M. Elferink, T. Henthorne, B. O'Rourke, and P. Kostka, "High efficiency natural gas fired 1 kWe thermoacoustic engine," submitted to *Appl. Energy* (2021).
10. M. A. G. Timmer, K. de Blok, and T. H. van der Meer, "Review on the conversion of thermoacoustic power into electricity," *J. Acoust. Soc. Am.*, Vol. 143 (2018), pp. 841-857.
11. R. S. Wakeland, "Use of electrodynamic drivers in thermoacoustic refrigerators," *J. Acoust. Soc. Am.,* Vol. 107 (2000), pp.827-832.
12. D. Gedeon, "DC gas flows in Stirling and pulse-tube cryocoolers," *Cryocoolers 9,* Plenum Press, New York (1997)*,* pp. 385-392.
13. M. Raefsky, "Fatigue properties of 17-4 PH and 15-5 PH steel in the H-900 and H-1050 condition," (1968), https://apps.dtic.mil/dtic/tr/fulltext/u2/691794.pdf, Boeing Vertol Co. Philadelphia PA.
14. G. W. Swift, D. L. Gardner, and S. Backhaus, "Acoustic recovery of lost power in pulse tube refrigerators," *J. Acoust. Soc. Am.*, Vol. 105 (1999), pp. 711-724.
15. T. W. Steiner, M. Hoy, G. D. S. Archibald, K. T. Gottfried, T. Kanemaru, and B. Medard de Chardon, "Apparatus and system for exchanging heat with a fluid," US patent application 2019/0033014 A1, (2019).
16. J. R. Olson and G. W. Swift, "Acoustic streaming in pulse tube refrigerators: tapered pulse tubes," *Cryogenics*, Vol. 37 (1997), pp. 769-776.
17. M. Dietrich, L. W. Yang, and G. Thummes, "High-power Stirling-type pulse tube cryocooler: Observation and reduction of regenerator temperature inhomogeneities," *Cryogenics*, Vol. 47 (2007), pp. 306-314.
18. J. H. So, G. W. Swift, and S. Backhaus, "An internal streaming instability in regenerators," *J. Acoust. Soc. Am.,* Vol. 120 (2006), pp. 1898-1909.